https://doi.org/10.1016/j.apenergy.2018.06.027

Study on an innovative three-dimensional wind turbine wake model

Haiying Sun, Hongxing Yang*

Renewable Energy Research Group, Department of Building Services Engineering, The Hong Kong Polytechnic University, Hong Kong

Abstract

In this paper, to help handle wind farm optimization problems, an original analytical three-dimensional wind turbine wake model is presented and validated. Compared with existing analytical wake models, the presented wake model also considers the wind variation in the height direction, which is more accurate and closer to the reality. The wake model is based on the flow flux conservation law, and it assumes that the wind deficit downstream of a wind turbine is Gaussian-shaped. The derivation process is described in detail. The wake model is validated by published wind tunnel measurement data at both horizontal and vertical sections. Detailed relative errors are analyzed: the relative errors are mostly within 5% in the horizontal profile validation and within 3% in the vertical profile validation. Based on the wake model, a series of prediction results from multiple views and at different positions are demonstrated. From the predictions, the three-dimensional wake model is effective in describing the spatial distribution of wind velocity. It makes a theoretical contribution to the single wake study, and it is also meaningful to the further study of multiple wakes. Because height is considered in the three-dimensional wake model, the model can be used to optimize wind turbine hub heights and to solve more wind farm layout optimization problems, which will further contribute to increasing the energy output and decreasing the cost of energy.

Keywords: Three-dimensional wake model; Derivation process; Wind tunnel validation; Wake distribution prediction.

1. Introduction

The wake effect appears in the wind flow field downstream of an operating wind turbine [1]. It is characterized by lower wind speeds and higher turbulence levels than the upstream conditions [2], and it causes the downstream wind to contain less energy than the upstream wind [3]. The wake spreads a long distance downstream of a wind turbine and returns to the surrounding wind gradually. This explains why on an operating wind farm, a wind turbine may be under the wake influence of more than one upstream wind turbine. If the wake effect is not evaluated properly, the overestimation of energy yields will cause a higher requirement of the electrical equipment's voltage level and the cables' capacity, influencing the operating reserve [4] and control strategy of the whole wind farm [5], which will finally induce a waste of investment on components' redundancy [6]. Many researchers have worked on wake models to assess the wake effect. Various developed wake models make it possible for scholars to carry out wind farm-related works. However, via comparisons among different wake models (six models of varying complexity [1], three commonly seen wake models [7], and a number of wake-induced turbulence models [8]), a crucial conclusion has been drawn that all wake models perform with high uncertainties [9]. As problems surface, challenges to the wake model issue are faced by researchers attempting to develop more accurate models.

The requirements of wake assessment methods are considerably distinct when handling different problems. Generally, wake models can be divided into analytical wake models [10] and numerical wake models [11]. Numerical wake models or more complicated analytical wake models are based on various theories, such as linear RANS (Ainslie [12] and Ott, et al. [13]), dynamic wake meandering (Larsen, et al. [14]), and the stochastic wake model (Manuel, et al. [15]). With development, the fidelities of these models continue to increase [16], which adds to the computational complexity and to the cost. These models can also estimate wind losses and wake distribution, but they are more widely used in aerodynamic analysis, blade structure studies, and mechanical loads [17]. For the wind farm layout

* Corresponding author. Tel.: 2766 5863
E-mail address: hong-xing.yang@polyu.edu.hk
The short version of the paper was presented at REM2017, October 18-20, Tianjin, China. This paper is a substantial extension of the short version of the conference paper

optimization process, the trial calculation of the optimal layout may be thousand times, and all wind directions should be involved in each calculation, a balance of accuracy and computation cost of estimating the wind loss is of critical importance The heavy computation cost of numerical wake models makes them impossible to apply to the wind farm layout optimization problem [18]; by contrast, analytical wake models are developed mainly to estimate the wind losses of the whole wind farm [19] because they are usually simple and have relatively high precision on wind speed deficit estimation.

The most widely used analytical wake model is the Jensen wake model [20], which is a one-dimensional (1-D) wake model. The Jensen wake model [21] (also called the Park model) is a preferential option for estimating the energy losses of a wind farm because of its simplicity and relatively high accuracy. The calculation based on the Jensen wake model has the lowest computation cost among wake models [22]. The Jensen wake model adopts the momentum conservation theory and assumes that the wake expands linearly after the upstream wind turbine [21]. It makes a good estimation of the energy content in the wake. However, according to this assumption, at any particular downstream distance, the inside wind velocity is seen to be constant across the wake plume, which is far from reality. Dufresne and Wosnik [23] studied the classical shear flow theories in the wakes, whereas Chamorro and Porté-Agel [24] organized wind tunnel experiments to study one single wind turbine's wind deficit. Both investigations found that after a certain downwind distance, the wind deficit is approximately Gaussian axisymmetric-shaped. The linear wake model was then further investigated. Recently, some two-dimensional (2-D) wake models were developed based on the Jensen wake model. Bastankhah and Porté-Agel [25] built the Bastankhah wake model in 2014, and the model was validated by a large-eddy simulation and experimental case studies. Although the wake model contains three variables, the wind distribution is only related to two factors, the downstream distance to the wind turbine and the distance to the hub axis. In 2015, Tian, et al. [26] developed a Cosine wake model in which the wind distribution on the horizontal plane is cosine-shaped. A similar principle Jensen-Gaussian wake model was then developed by Gao, et al. [27] in 2016, in which the wind distribution is as its name describes, Gaussian-shaped.

Admittedly, the 2-D wake models are more effective in forecasting wind losses than the Jensen wake model, but practical limitations remain. 2-D wake models do not consider the wind velocity variation in the height direction, the spatial optimization problems are tough or even more serious than before. Because a great number of wind farms are built in rugged and uneven areas, the wind turbines are not actually fixed in the same horizontal plane. The 2-D wake models simplify the wind farm layout optimization to a plane problem, which is apparently unreasonable. Furthermore, some research has focused on nonuniform wind farm optimization problems. Chen, et al. [28] pointed out that the power output will increase by using wind turbines with different hub heights when the total number of wind turbines is the same. Feng and Shen [29] investigated the design of offshore wind farms with multiple types of wind turbines and hub heights and found that a nonuniform wind farm can achieve a lower levelised cost of energy. Nonuniform wind farm optimizations should not neglect the factor of height difference. The 2-D wake models are not sufficiently complete and cannot well support further investigation of the nonuniform problem. In addition, the trend of power upsizing of single wind turbines dramatically increases the hub height and the rotor diameter; the height distance and the wind speed difference in the swept area also increase correspondingly. The 2-D wake models' uniform wind assumption in the height direction ignores these differences, which causes huge errors when estimating the energy output and is no longer applicable. As a result, 2-D wake models cannot provide comprehensive and complicated spatial wind farm optimization anymore. The further development of an analytical wake model from 2-D to three-dimensional (3-D) is significant and necessary.

In this paper, a new 3-D wake model is presented to include height consideration. In section 2, the assumptions and derivation process are explained in detail. The analytical expression of the wind distribution in the space is given out. In section 3, the validation of the wind tunnel measurement data demonstrates the accuracy of the new model. The vertical profile validation especially affirms the practicality of applying the model to the wind farm height and spatial optimization. In section 4, predictions of the 3-D wake model from multiple views and at different positions are demonstrated. These predictions show that it is feasible and practical to apply the 3-D wake model to depict the spatial wind distribution. Finally, in section 5, key findings of this study are summarized. With the 3-D wake model, the wind speed at each position can be calculated simply. The wind variation in the height direction can also be demonstrated clearly. The 3-D wake model can be applied in wind farm layout design problems to make the estimation of the energy output more accurate. It can also handle wind turbine height optimization problems and nonuniform wind farm optimization problems. This 3-D wake

model is more appropriate to the modern wind farm and will contribute to increasing the energy utilization ration and decreasing the energy cost.

Nomenclature

a	axial induction factor	$r_w(x)$	wake-influenced radius (m)
$A(x)$	parameter in 3-D wake model (m^2)	$S_{r_w(x)}$	circular area with radius $r_w(x)$ (m^2)
$B(x)$	parameter in 3-D wake model (m/s)	S_{r_0}	circular area with radius r_0 (m^2)
C	parameter in 3-D wake model	u_0	wind speed measured at z_0 height (m/s)
h_0	wind turbine hub height (m)	$U(x)$	wind velocity in 1-D wake model (m/s)
I_0	incoming free stream turbulence intensity	$U(x,r)$	wind velocity in 2-D wake model (m/s)
I_{wake}	wake turbulence intensity	$U(x,y,z)$	wind velocity in 3-D wake model (m/s)
k_0	rate of the wake expansion	$U_0(z)$	incoming wind speed distribution (m/s)
k_{wake}	wake decay constant	v_0	average wind speed just behind the wind turbine (m/s)
$Q(x)$	total flow flux (m^3/s)	z_0	reference height (m)
r	radial distance to the centerline (m)	α	wind speed power law parameter
r_0	wind turbine rotor radius (m)	$\sigma(x)$	parameter in 3-D wake model (m)

2. Derivation of the three-dimensional wake model

2.1 Introduction of the three-dimensional wake model

Figure 1 shows schematic diagrams of 1-D and 2-D wake models. In the 1-D wake model, the incoming wind is assumed to be evenly distributed and the downwind wind velocity $U(x)$ is only relative to the downstream distance x. In the 2-D wake model, the incoming wind is also assumed to be evenly distributed, whereas the wind deficit is assumed to be Gaussian-shaped. The actual wind velocity $U(x,r)$ in the 2-D wake model is relative to the downstream distance x and the radial distance to the centerline r. However, as matter of fact, the downstream wind distribution is complicated and absolutely beyond the 2-D distribution.

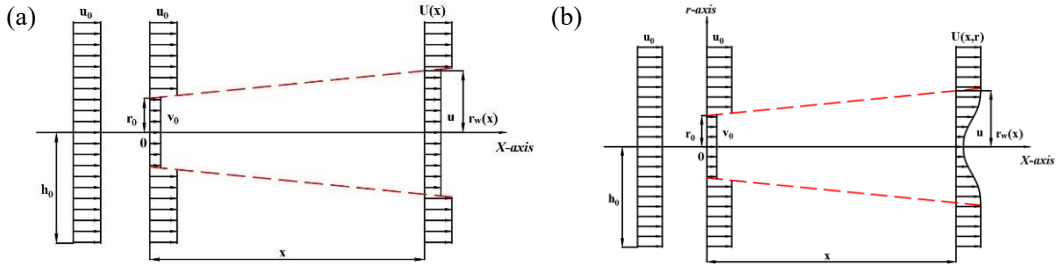

Figure 1 Schematic diagrams of analytical wake models: (a) 1-D wake model; and (b) 2-D wake model.

Figure 2 demonstrates a schematic diagram of the proposed 3-D wake model. In this 3-D wake model, the wake-influenced radius $r_w(x)$ varies along the downstream distance x; the wind deficit is Gaussian-distributed in the 3-D space rather than linearly distributed. Most importantly, this 3-D wake model assumes that the incoming wind distribution $U_0(z)$ varies along the height direction, and the variation is accounted for from the beginning of the derivation process. Therefore, the wind velocity $U(x,y,z)$ is relative to the X, Y, and Z directions. The X axis and Z axis are shown in Figure

2; the Y axis is perpendicular to the paper and points into it.

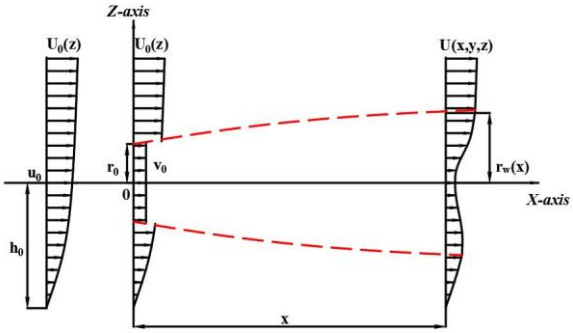

Figure 2 Schematic diagram of the 3-D wake model.

The assumption of the 3-D wake model is closer to reality and has not been adopted in any other analytical wake model. With the proposed 3-D wake model, it is easy to obtain the wind velocity $U(x,y,z)$ of any spatial position downstream of a wind turbine.

2.2 Assumptions of the three-dimensional wake model

There are three basic assumptions of the newly presented 3-D wake model.

The first assumption is that the wind velocity deficit at downstream distance x is Gaussian-distributed, which is expressed as $A(x)(\frac{1}{2\pi\sigma(x)^2}e^{-\frac{y^2+(z-h_0)^2}{2\sigma(x)^2}})+B(x)$. The incoming wind speed distribution is expressed by $U_0(z)$. Consequently, the actual wind velocity $U(x,y,z)$ at the downstream position can be described by equation (1).

$$U(x,y,z)=A(x)(\frac{1}{2\pi\sigma(x)^2}e^{-\frac{y^2+(z-h_0)^2}{2\sigma(x)^2}})+B(x)+U_0(z) \tag{1}$$

In the equation, h_0 is the wind turbine hub height. $A(x)$, $B(x)$, and $\sigma(x)$ are three important parameters that decide the Gaussian shape of the wind deficit. To simplify the calculation, $\sigma(x)$ is defined as $\sigma(x)=\frac{r_w(x)}{C}$, in which C is a constant and is to be determined according to the real operating conditions. In the 3-D wake model, $A(x)$ and $B(x)$ vary along the downstream distance and their derivation processes will be introduced in a following study.

The second assumption is based on the momentum conservation theory, which refers to the Jensen wake model [21], and it means that the flow flux is conservative in a specific area at any wake section.

A circular area with radius $r_w(x)$ is chosen to calculate the total flow flux $Q(x)$. At the plane just behind the wind turbine, the total flow flux $Q(x)$ is calculated from equation (2). $Q(x)$ consists of two parts: one is the flow flux within the circular area of rotor radius $\pi r_0^2 v_0$ and the other one $\iint_{S_{r_w(x)}-S_{r_0}} U_0(z)ds$ is the flow flux beyond the circular area but within another circular area with radius $r_w(x)$.

$$Q(x)=\pi r_0^2 v_0+\iint_{S_{r_w(x)}-S_{r_0}} U_0(z)ds \tag{2}$$

In equation (2), r_0 is the rotor radius of the wind turbine and v_0 is the average wind speed just behind the wind turbine. In reference [21], v_0 is one third of the ambient wind velocity in accordance

with classical theory. Therefore, in this study, v_0 is similarly assumed to be one third of the incoming wind speed at the hub height of the wind turbine. $S_{r_x(x)}$ is the circular area with radius $r_w(x)$, whereas S_{r_0} is the circular area with the rotor radius r_0.

At the plane downstream of the wind turbine at x distance, the total flow flux $Q(x)$ is calculated from equation (3), which is the integration of the wind velocity $U(x,y,z)$ at the circular area within the radius $r_w(x)$.

$$Q(x) = \iint_{S_{r_w(x)}} U(x,y,z)ds \tag{3}$$

Then, combining equation (2) and equation (3), the final expression of the second assumption is shown as equation (4).

$$\pi r_0^{\,2} v_0 + \iint_{S_{r_w(x)} - S_{r_0}} U_0(z)ds = \iint_{S_{r_w(x)}} U(x,y,z)ds \tag{4}$$

The third assumption is that the wind velocity is continuous at the wake boundary. Therefore, this assumption can be expressed by equation (5).

$$\frac{A(x)}{2\pi\sigma(x)^2} e^{-\frac{y^2+(z-h_0)^2}{2\sigma(x)^2}} + B(x) + U_0(z) = U_0(z) \quad , where \quad y^2 + (z-h_0)^2 = r_w(x)^2 \tag{5}$$

2.3 Derivation process

In this study, the anemometer height and the wind turbine hub height are also considered. To calculate the wind speed variation along the vertical direction, the wind power law is applied. The incoming wind speed distribution $U_0(z)$ is expressed by equation (6) [30].

$$U_0(z) = u_0 \cdot \left(\frac{z}{z_0}\right)^{\alpha} \tag{6}$$

where z_0 is the reference height and u_0 is the wind speed measured at the height of z_0, whereas α is the wind speed power law parameter whose referent value can be found in [31].

The first step is to calculate the flow flux $Q(x)$ behind the wind turbine according to a series of equations [equation (7)].

$$\begin{cases} Q(x) = \pi r_0^{\,2} v_0 + \iint_{S_{r_w(x)} - S_{r_0}} U_0(z)ds \\ v_0 = (1-2a)u_0 \\ U_0(z) = u_0 \left(\frac{z}{z_0}\right)^{\alpha} \\ r_w(x) = r_0 + k_{wake} \cdot x \end{cases} \tag{7}$$

In the above equations, a is the axial induction factor and k_{wake} is the wake decay constant, which can be estimated according to equation (8).

$$k_{wake} = k_0 \frac{I_{wake}}{I_0} \tag{8}$$

The term k_0 is the rate of the wake expansion, which is recommended to be 0.075 for onshore wind turbines [32] and 0.04 or 0.05 for offshore wind turbines [33]; I_0 is the incoming free-stream turbulence intensity and I_{wake} is calculated according to equations (9) and (10) [34].

$$I_{wake} = \sqrt{I_0^{\,2} + I_+^{\,2}} \tag{9}$$

$$I_{+} = 0.73a^{0.8325} I_0^{\,0.0325} \left(x/D\right)^{-0.32} \tag{10}$$

The next step is to solve $A(x)$ and $B(x)$ based on another series of equations [equation (11)].

$$\begin{cases} \dfrac{A(x)}{2\pi\sigma(x)^2} e^{-\frac{y^2+(z-h_0)^2}{2\sigma(x)^2}} + B(x) + U_0(z) = U_0(z) \quad , where \quad y^2 + (z-h_0)^2 = r_w(x)^2 \\ Q(x) = \iint\limits_{S_{r_w(x)}} U(x,y,z)ds \\ U(x,y,z) = A(x)\left(\dfrac{1}{2\pi\sigma(x)^2} e^{-\frac{y^2+(z-h_0)^2}{2\sigma(x)^2}}\right) + B(x) + U_0(z) \\ \sigma(x) = \dfrac{r_w(x)}{C} \end{cases} \tag{11}$$

Put $Q(x)$, solved from equation (7), into (11); then only $A(x)$, $B(x)$, and C are unknown. Finally, $A(x)$ and $B(x)$ can be expressed by constant C as equation (12).

$$\begin{cases} A(x) = \dfrac{Q(x) - \int_{h_0 - r_w(x)}^{h_0 + r_w(x)} 2\sqrt{r_w(x)^2 - (z-h_0)^2} \cdot U_0(z)dz}{\left(1 - e^{-\frac{C^2}{2}} - \dfrac{C^2}{2} \cdot e^{-\frac{C^2}{2}}\right)} \\ B(x) = -\dfrac{A(x) \cdot C^2}{2\pi r_w(x)^2} \cdot e^{-\frac{C^2}{2}} \end{cases} \tag{12}$$

C is an empirical parameter that will influence the wind deficit in the wake. In the 2-D Jensen–Gaussian wake model [27], C is suggested to be 6.6564 in one case. However, wind deficit is actually affected by many factors, such as the blade shape, the incoming wind speed, and the turbulence intensity. Therefore, in this study, it is recommended that C be set to different values according to the operating conditions.

In addition, in equation (6), $U_0(z) = u_0 \cdot \left(\dfrac{z}{z_0}\right)^{\alpha}$ is just one of the expressions of the incoming wind distribution. In the 3-D wake model, some other expressions of $U_0(z)$ can also be applied.

3. Validation of the three-dimensional wake model

To validate the proposed 3-D wake model, published wind tunnel measurement data are cited in this study to test the accuracy of the model. Both the horizontal and the vertical wake profile validations show the good effectiveness of the proposed 3-D wake model.

3.1 Validation with the horizontal wake profile

3.1.1 Wind tunnel measurement data

The adopted horizontal wake profiles were published by reference [35]. In 1989, Hassan made an intensive analysis of wind turbine wake at the Marchwood Engineering Laboratory's atmospheric boundary-layer wind tunnel. The analysis used 1/160th-scale horizontal axis wind turbines, which had realistic performance properties and sophisticated data logging components. This analysis process generated comprehensive data on the turbulent and mean flow downstream of single and multiple wind turbines. The model site was flat with artificial surface roughness. The artificial surface roughness in the wind tunnel was uniform and the roughness length was 0.075 m.

As for the wind turbines, the rotor diameter of the 1/160th-scale models was 0.27 m; the corresponding full-scale rotor diameter was 43.2 m. The assumed wind turbine hub height was 50 m, where the free wind speed was 5.3 m/s. The model turbines were operated at three ratios of tip speed. In

this validation, the model tip speed ratio was chosen as 2.9, with a 6.78 rpm rotor speed. Corresponding to this operating condition, the constant C in the 3-D wake model was set as $C=1.98$.

3.1.2 Result comparisons

Figure 3 shows the horizontal wake profile comparisons of the 3-D wake model and the wind tunnel measured data. Figure 3(a) is at a 5D downstream distance and Figure 3(b) is at a 10D downstream distance (D represents the rotor diameter of the wind turbine). In the figures, the blue lines represent the prediction results from the 3-D wake model; the red dots represent the wind tunnel measured data. The horizontal axis is the dimensionless ratio of y distance and rotor diameter D. The vertical axis is the ratio of wind velocity $U(x,y,z)$ and the incoming wind speed at wind turbine hub height u_0.

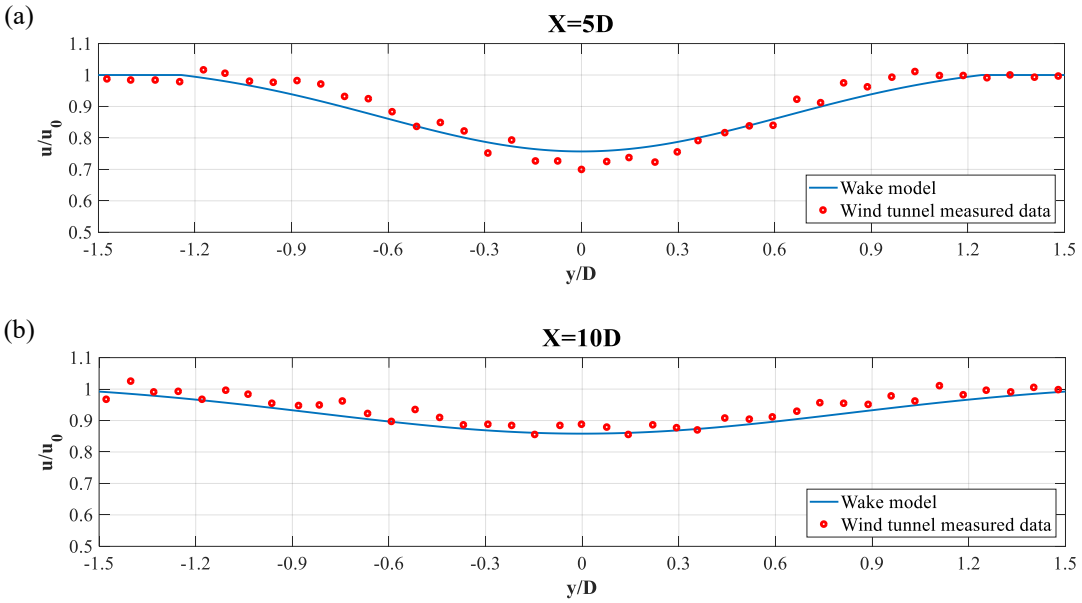

Figure 3 Horizontal results comparisons of the measurement data and 3-D wake model-predicted wind velocity at specific downstream distances: (a) $x=5D$; and (b) $x=10D$.

From the wake profiles, the presented 3-D wake model apparently predicts the wind velocity well in the horizontal direction at the given wind turbine hub height. At the 5D downstream distance, the wind velocity predicted by the 3-D wake model is greater than that measured at the centerline around but lower than that measured at the y/D ratio range of $\pm(0.5\sim1)$. At the 10D downstream distance, the 3-D wake model predicts greater wind velocities at most measured positions, but the errors are much smaller. Generally, the 3-D wake model is more accurate at the 10D downstream distance.

The specific relative errors of the comparison results are also analyzed. A total of 41 points are compared according to the wind tunnel experiments. Figure 4 shows the error analysis of the comparison results at the 5D and 10D downstream distances.

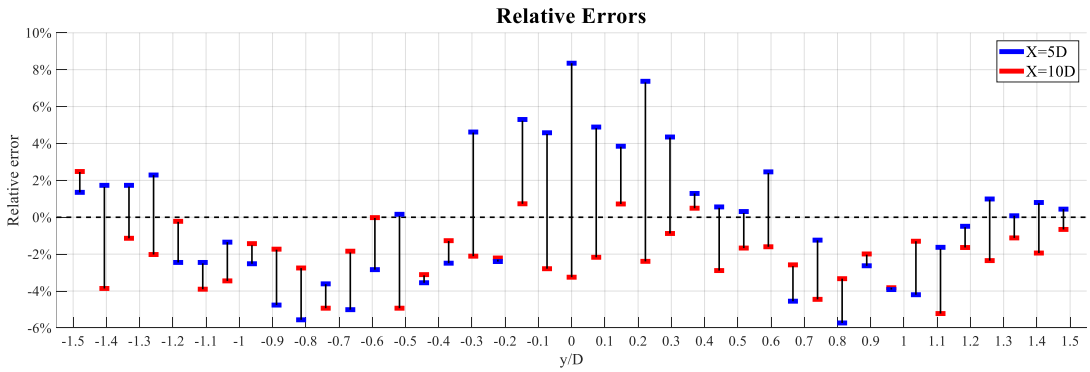

Figure 4 Relative errors of horizontal profiles.

From the error analysis, the results predicted by the 3-D wake model agree well with the measurement data. The largest error is 8.35% in the 5D downstream distance. Only two errors are beyond ±6%, and other errors are mostly within ±5%. Some large errors are centralized within the $\pm 0.3D$ area, which shows that the 3-D wake model seems to be somewhat inaccurate in the center wake-influenced area. The reason may be that huge turbulence intensity appears in the center area, and the 3-D wake model as a simple analytical wake model cannot predict the turbulence well. By contrast, the errors at the 5D distance are larger than those at the 10D distance. The wake model predictions are more accurate at far downstream distance areas. It should also be noted that apart from the center area, most errors are negative, which indicates that the 3-D wake model is likely to predict wind velocities lower than the reality at distances far from the center area. In addition, theoretically, the wind velocity at the lateral areas that are not under the wake effect should be the same as the incoming wind velocity, namely, the same as the wake model predictions. However, some unstable errors appear in the lateral area, which implies that errors may exist in the measurement data and that the experimental errors may also influence the verification of the wake model.

3.2 Validation with the vertical wake profile

3.2.1 Wind tunnel measurement data

The adopted vertical wake profile data were published by reference [36]. The test was conducted in the atmospheric boundary-layer wind tunnel at St. Anthony Falls Laboratory. The high-resolution measurement data of the wind distribution downstream a miniature wind turbine were collected by hot-wire anemometry.

In the experiment, a three-blade GWS/EP-6030×3 rotor was fixed on the wind turbine model and linked with a small DC generator motor. The rotor diameter was 0.150 m and the hub height was 0.125 m. The motor was cylindrically shaped, with a length $l_m = 0.03m$ and a diameter $d_m = 0.015m$. The turbine tower was also cylindrically shaped, with a length $l_m = 0.118m$ and a diameter $d_m = 0.005m$. The boundary-layer flow was characterized by a freestream speed of 2.8 m/s and the boundary-layer depth was 0.46 m. The size of the wind tunnel was 16 × 1.7 × 1.7 m, and the boundary layer was built at the end of the wind tunnel section in the downwind direction. The incoming velocity at the hub height of the miniature wind turbine was 2.2 m/s and the wind speed power law parameter α was 0.15. Corresponding to this operating condition, in this validation, the constant C in the 3-D wake model was set as $C = 5.15$.

3.2.2 Result comparisons

Figure 5 shows the vertical wake profile comparisons of the wake model predictions and the wind tunnel measured data at various downwind distances. The wake profiles are in the wind turbine section, which is also the $y = 0$ section. Figure 5(a) shows the incoming wind distribution; (b) is at the $x = 5D$ downstream distance; (c) is at the $x = 7D$ downstream distance; (d) is at the $x = 10D$ downstream distance; (e) is at the $x = 14D$ downstream distance, and (f) is at the $x = 20D$ downstream distance. In the figure, the horizontal axis is the wind velocity $U(x, y, z)$ and the vertical axis is the dimensionless ratio of z distance and wind turbine rotor diameter D.

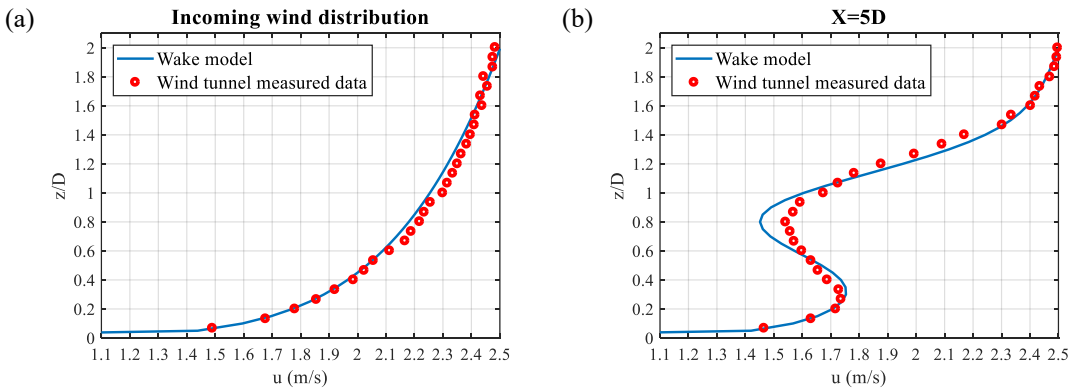

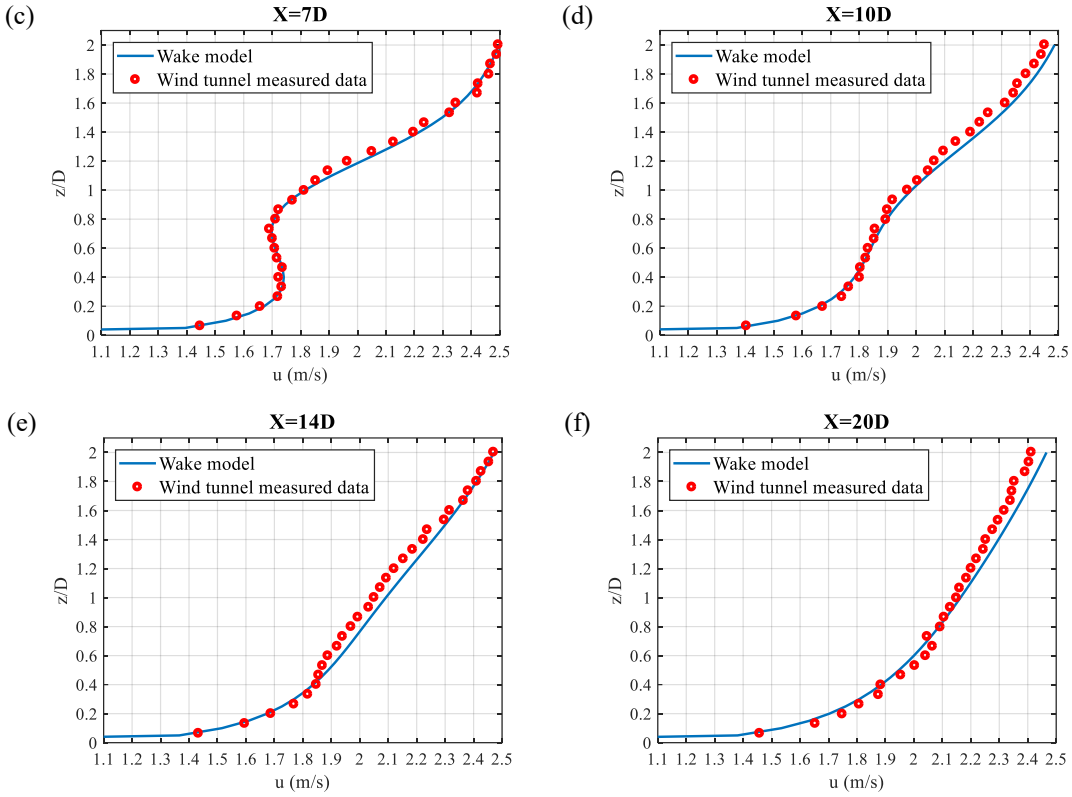

Figure 5 Vertical results comparisons of the measurement data and the 3-D wake model predicted wind velocity at specific downstream distances: (a) incoming wind distribution; (b) $x=5D$; (c) $x=7D$; (d) $x=10D$; (e) $x=14D$; and (f) $x=20D$.

From the vertical wake profiles, it is obvious that the proposed 3-D wake model can also predict the wake distribution well in the vertical direction at the wind turbine section. For the incoming wind, the wake model slightly underestimates the wind velocity in the mid-height positions. The predicted wind speeds agree well in all downstream distance positions, especially at the low height position under a 0.4 z/D ratio. At the 5D downstream distance, the wake model underestimates the wind velocity at around the wind hub height position, where the largest error seems to lie. In most other situations, the wake model slightly overestimates the wind velocity. The specific error analysis of the vertical wind profile comparison results is shown in Figure 6, in which 30 measurement points are compared.

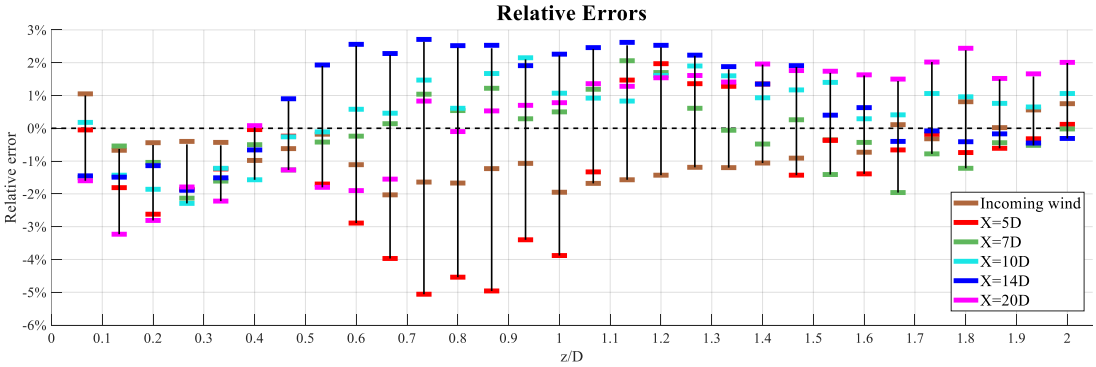

Figure 6 Relative errors of vertical profiles.

The error analysis further verifies the effectiveness of the proposed 3-D wake model. From the results, the largest error is 5.06% at the $x=5D$ downstream distance and only five errors are larger than 4%, also at the $x=5D$ downstream distance, whereas most errors are within ±3%. The predictions at positions near the hub height area tend to have large errors, which is similar to the results of the horizontal analysis, and the rough estimation of the turbulence may be responsible for this finding. It is noteworthy that the wake model tends to underestimate the wind velocity for the incoming wind and the

small downstream distance of $5D$ in this study, but it tended to overestimate it at most other downstream positions. Attention should be paid to this problem when applying the 3-D wake model, and further study should be concentrated on it. Where the incoming wind is totally free from the wake effect, the wake model tends to underestimate the wind velocity, although the largest error is just 2.03%. A more accurate incoming wind speed formula would perform better and should be adopted if necessary.

Because the selected measurement data are from wind tunnel tests, some experimental errors may have affected the results. In Figure 3, the measurement data are not symmetrical around the center line; in Figure 5, the wind distributions in the high positions of different downstream distances, where the wind is not under wake's effect, are not quite coincident theoretically. These errors may be caused by some experimental factors, and they have an effect on the validation of the wake model. However, the overall results show that good consistency remains between the 3-D wake model and the wind tunnel measurement data from both the horizontal and vertical wind profiles. Therefore, it is reliable to apply the proposed 3-D wake model to predict any downwind spatial position's wind velocity. In contrast, more comprehensive and accurate wind field tests are necessary to further check the effectiveness of this wake model.

4. Predictions of the three-dimensional wake model

Application of the 3-D wake model to predict the wind velocity of a specific point (x, y, z) includes three main steps. The first is to determine the relevant parameters according to the operating conditions and the incoming wind distribution. The second is to calculate the distance from the point to the centerline r according to equation (13) and then to judge whether the point is under the wake effect according to the equation $r_w(x) = r_0 + k_{wake}x$. The third step is to calculate the wind velocity according to the judgment of step 2. If $r_w(x) < r$, the point is not within the wake-influenced zone and the wind velocity can be calculated simply by equation (6); if $r_w(x) > r$, the point is in the wake-influenced zone and the wind velocity should be calculated from the 3-D wake model as introduced in section 2.3.

$$r = \sqrt{y^2 + (z - h_0)^2} \tag{13}$$

With the validated 3-D wake model, it is more convenient to study the wake distribution and wake performance in the whole spatial view. In this chapter, a case of multiple views of a wind turbine's wake profile is demonstrated. The rotor radius r_0 is 15 m, the hub height h_0 is 50 m, the incoming wind speed at the hub height is 4 m/s, and the wind speed power law parameter is 0.1. The incoming wind is described by equation (6).

4.1 Wake profiles from the Y–Z view

Figure 7 shows the Y–Z view of the wind profile: (a) is the incoming wind distribution; (b) is at the $x = 2.5D$ downstream distance; (c) is at the $x = 5D$ downstream distance; (d) is at the $x = 10D$ downstream distance; (e) is at the $x = 15D$ downstream distance, and (f) is at the $x = 20D$ downstream distance. The horizontal axis represents the y distance, which ranges from 0 m to 150 m. The vertical axis represents the height, which ranges from 0 m to 120 m. The wind velocity is represented by different colors, which refer to the color bar to the right of each figure.

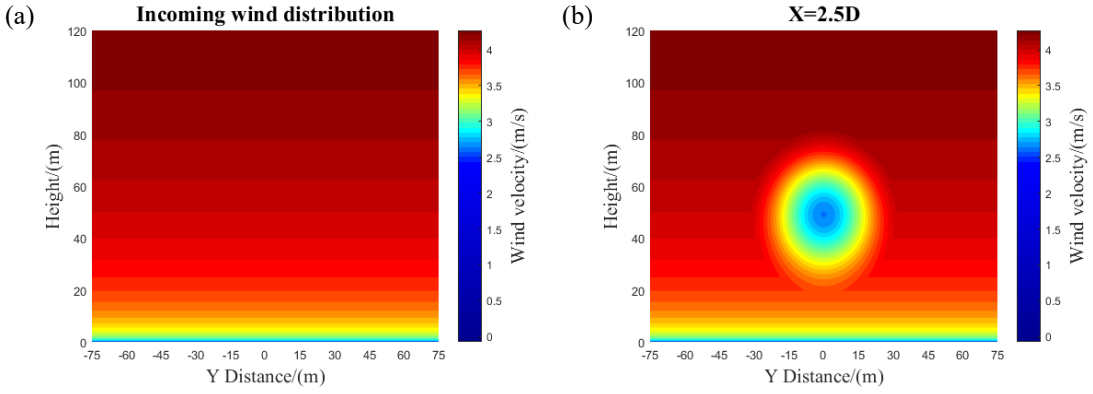

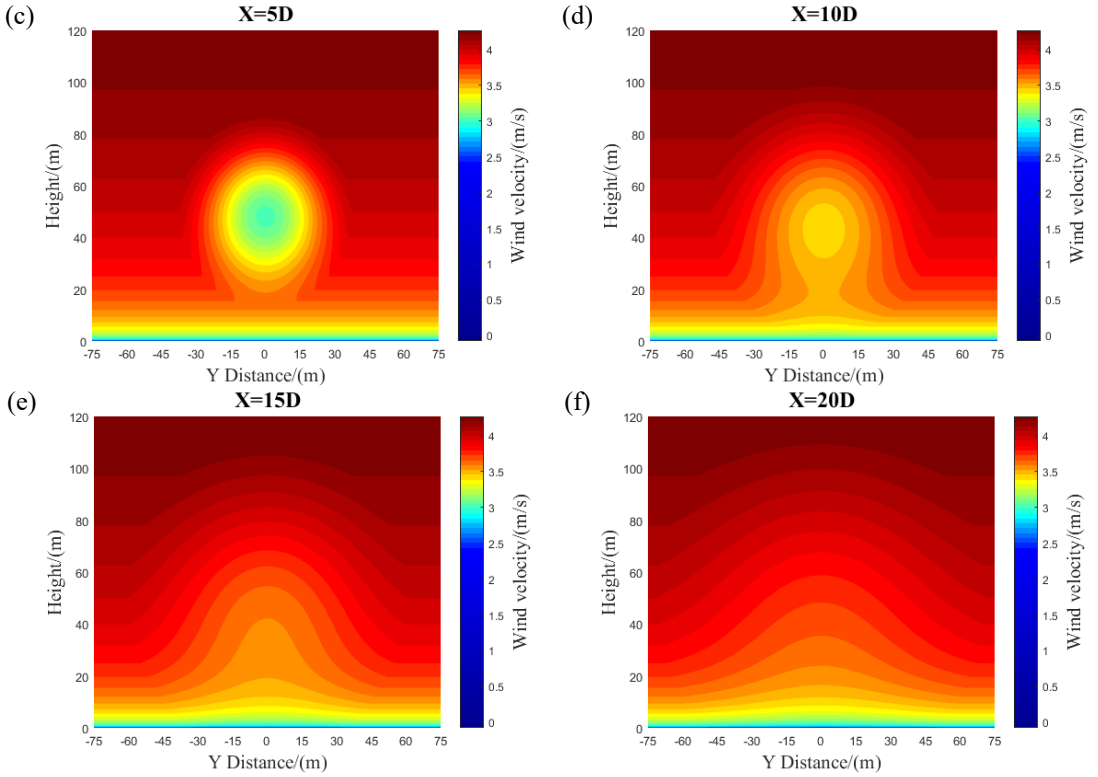

Figure 7 Y–Z views of the wind profile at different positions: (a) incoming wind distribution; (b) $x = 2.5D$; (c) $x = 5D$; (d) $x = 10D$; (e) $x = 15D$; and (f) $x = 20D$.

From the results, the wake-influenced area expands with the increase of the downstream distance at the same time the wind deficit phenomenon is weakened. This can be explained by the flow flux conservation law. However, it is clear that the wind deficit is not uniformly distributed in any part of the wake-influenced area. In contrast, with expansion of the wake circle, the wake distribution along the height cannot be ignored unconditionally. Within the 5*D* downstream distance, the wind speed can still be estimated by a particular simple shape, like a Gaussian shape. However, after the 5*D* distance, from the figure, the wind speed distribution becomes more complicated, and it is not suitable to apply the original method. It can be seen that the downstream wind distribution is neither the simple uniform distribution predicted by the 1-D wake model nor a simple shape distribution, like a Gaussian or cosine shape, as some 2-D wake models predict. Therefore, application of the proposed 3-D wake model is necessary.

4.2 Wake profiles from the X–Z view

Figure 8 shows X–Z views of the wind profile at different positions along the Y distance: (a) is the wind turbine section; (b) is the $y = 0.2D$ section; (c) is the $y = 0.4D$ section; (d) is the $y = 0.6D$ section; (e) is the $y = 0.8D$ section, and (f) is the $y = 1.0D$ section. Because the wake distribution is symmetric about the wind turbine section, half-views from one side of the symmetric section are enough to describe the wake distribution. From these X–Z view results, the wake profile is clearer and more stereoscopic.

At the wind turbine position, the wake effect is serious within 120 m, equivalent to 4*D*, in the X downstream distance. As the Y distance from the wind turbine position increases, the serious wake-influenced range is narrowed. Therefore, when designing a wind farm, the minimum distance between any two wind turbines should be no less than 4*D*. It can also be seen that the downstream wind distribution along the height direction is also influenced by the wake effect. In most wind farm layout studies, as 1-D or 2-D wake models are adopted, each wind turbine is considered to have the same incoming wind condition, which is not appropriate. Especially for large wind turbines, the wake effect is more serious and the wake-influenced range is even wider. Considering the wake effect on each wind turbine's incoming wind is of great importance. Consequently, height optimization also deserves to be included in wind farm layout considerations.

(a)

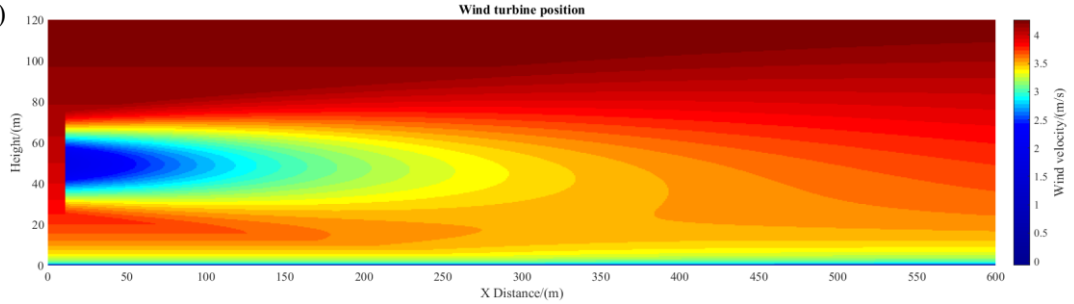
Wind turbine position
Height/(m)
X Distance/(m)
Wind velocity/(m/s)

(b)

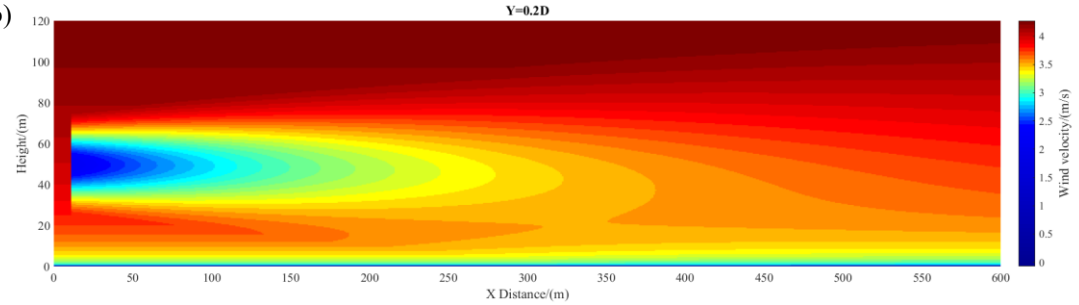
Y=0.2D
Height/(m)
X Distance/(m)
Wind velocity/(m/s)

(c)

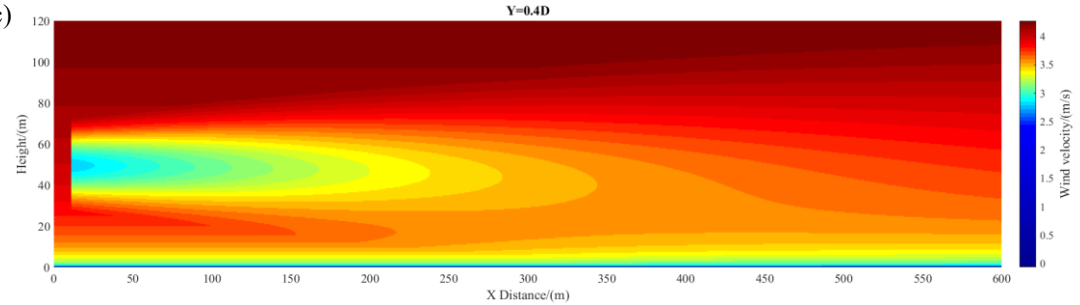
Y=0.4D
Height/(m)
X Distance/(m)
Wind velocity/(m/s)

(d)

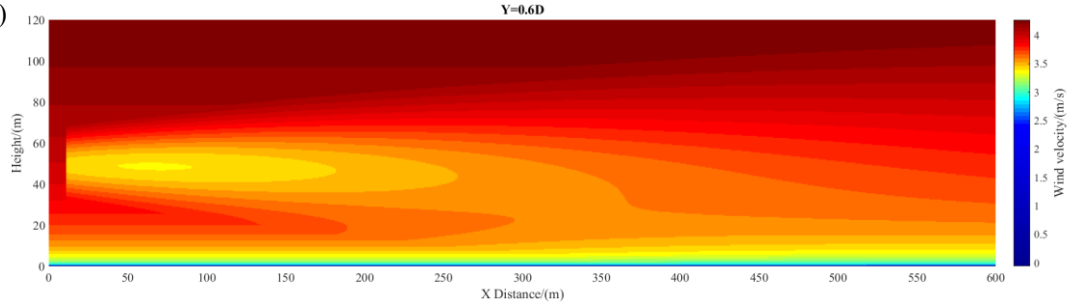
Y=0.6D
Height/(m)
X Distance/(m)
Wind velocity/(m/s)

(e)

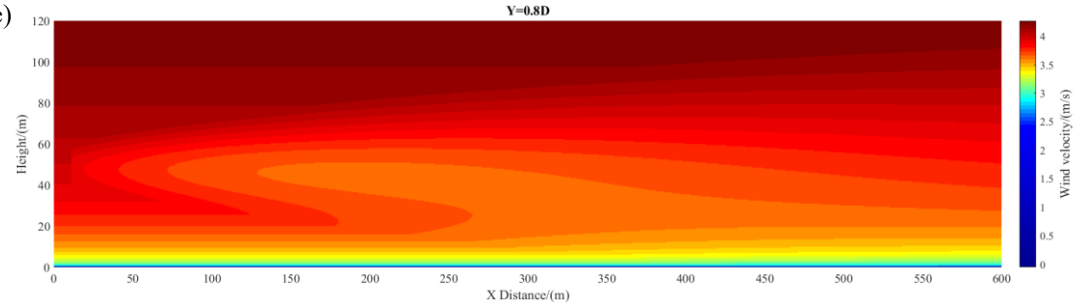
Y=0.8D
Height/(m)
X Distance/(m)
Wind velocity/(m/s)

(f)

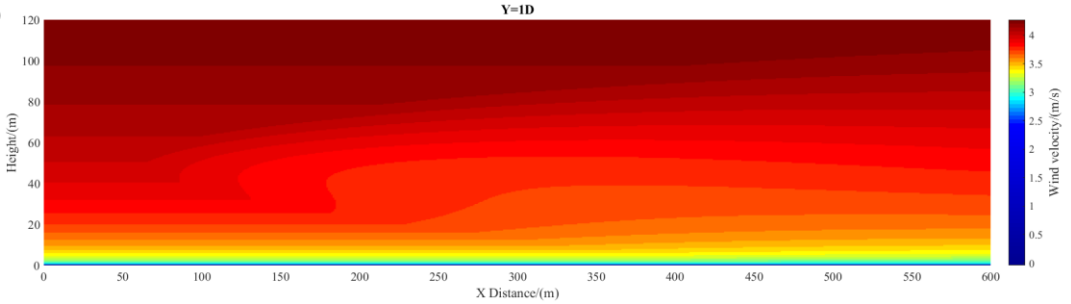

Figure 8 X–Z views of the wind profile at different positions: (a) wind turbine position; (b) $y=0.2D$; (c) $y=0.4D$; (d) $y=0.6D$;.(e) $y=0.8D$; and (f) $y=1D$.

It is noteworthy that the wake estimation at the space near the wind turbine and ground may be far from reality. This is because in the mentioned space, the viscosity causes huge turbulence, which is not considered in the 3-D wake model. Actually, this simplification will hardly affect the wind farm layout because the wind turbines will not be fixed that close to each other or near the ground. Not much turbulence will have a far-reaching effect on the downstream wind turbine, so it is tolerable to not include that turbulence in the consideration of wind farm energy loss problems.

4.3 Wake profiles from the X–Y view

Figure 9 shows X–Y views of the wind profile at different positions in the height direction: (a) is the $Height=h_0+1D$ section; (b) is the $Height=h_0+0.5D$ section; (c) is the $Height=h_0$ section; (d) is the $Height=h_0-0.5D$ section, and (e) is the $Height=h_0-1D$ section.

Because the effect that wind varies in the height direction is considered, it is clear that the wind distributions at various heights are not symmetrical to the wind turbine hub height plane. It can be inferred that each horizontal plane has a unique distribution of the wake and that both the wake boundary and the wake intensity are different.

(a)

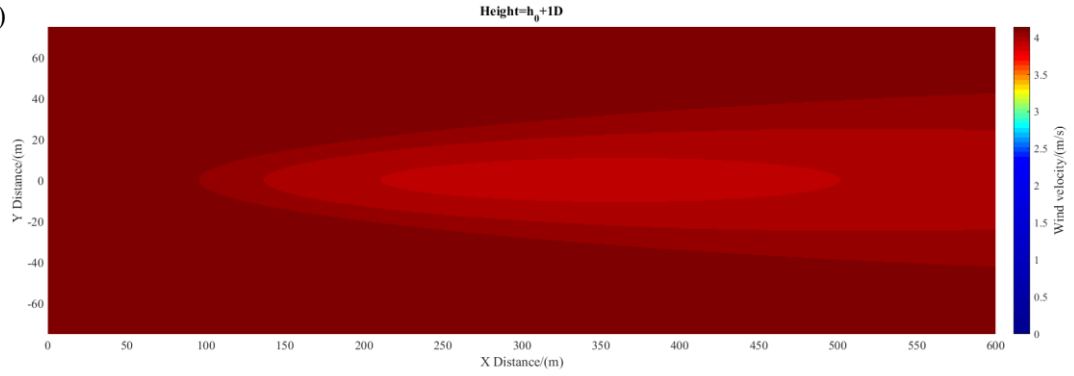

(b)

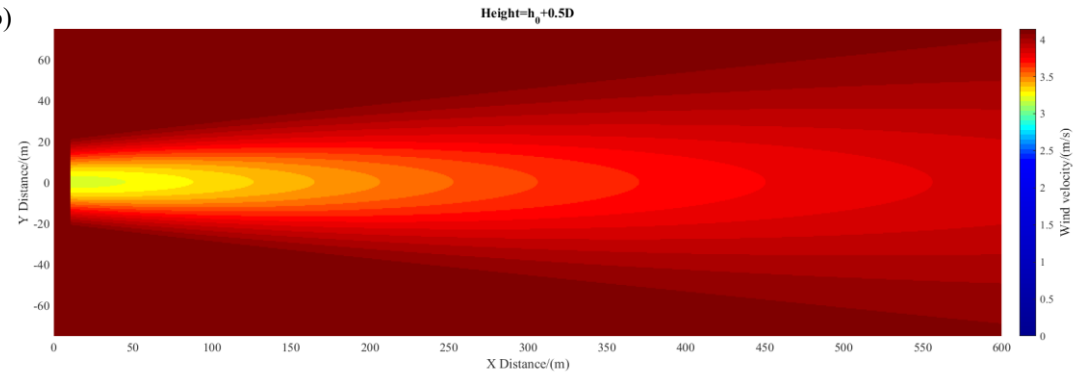

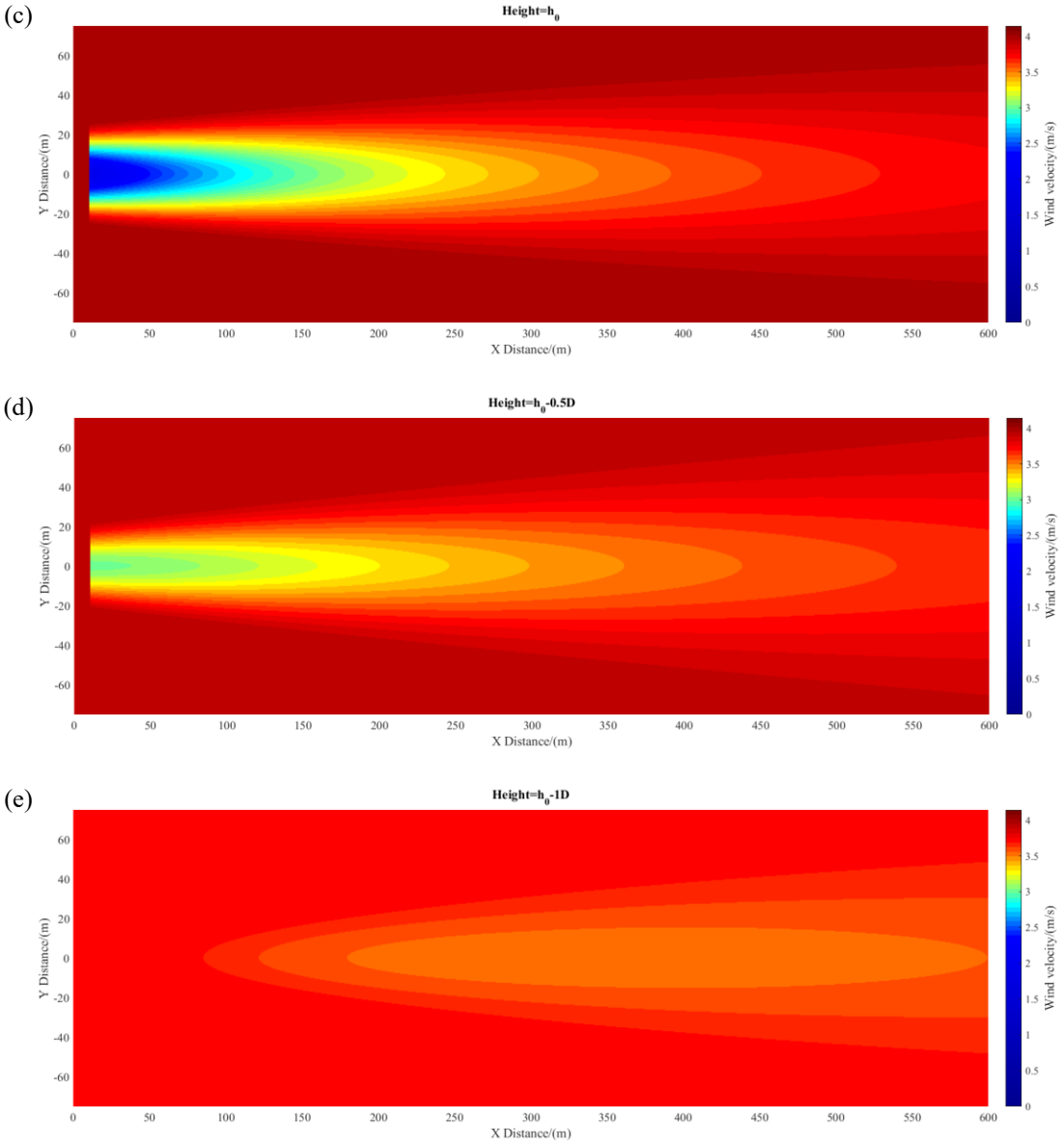

Figure 9 X–Y views of the wind profile at different positions: (a) $Height = h_0 + 1D$; (b) $Height = h_0 + 0.5D$; (c) $Height = h_0$; (d) $Height = h_0 - 0.5D$, and (e) $Height = h_0 - 1D$.

The demonstration of wake profiles from the three views show the effectiveness of the 3-D wake model. It can forecast the wind distribution at any position either before or after the wind turbine, within or without the wake boundary. Especially in the height direction, the superiority of the 3-D wake model is obvious.

5. Conclusions

In this paper, a novel analytical 3-D wake model is presented to help describe the wind distribution in space at a wind farm. The main conclusions are summarized as follows:

(1) The wake model is based on the momentum conservation theory and assumes that the wind deficit is Gaussian-shaped and the wind velocity is continuous at the wake boundary. It can calculate the wind velocity at any spatial position with high accuracy and little computational cost. The wake model considers the height direction's influence, which makes it more advanced than other analytical wake models.

(2) Wind tunnel measurement data were used to validate the 3-D wake model. In the validation of

the horizontal wake profile, the largest error was 8.35%, most errors were within ±5%, and some large errors were centralized within the $\pm 0.3D$ area. Apart from the center area, most errors were negative, which indicates that the 3-D wake model is likely to predict wind velocities smaller than the reality at distances far from the center area. In the validation of the vertical wake profile, the largest error was 5.06%, most errors were within ±3%, and the predictions at positions near the hub height area tended to have large errors. The wake model tended to underestimate the wind velocity for the incoming wind and the small downstream distance, but it tended to overestimate it at most other downstream positions. The 3-D wake model, as a simple analytical wake model, cannot predict the turbulence well, but its predictions are quite accurate far downstream beyond the 5D downstream distance. In addition, according to the analysis, some experimental errors affected the validation of the wake model to some extent.

(3) A series of Y–Z view, X–Z view, and X–Y view wake profiles predicted by the 3-D wake model were demonstrated. From the Y–Z view, the wake-influenced area expanded with the increase of the downstream distance, and the wind deficit phenomenon was also weakened. The wind deficit is not uniformly distributed in the wake-influenced area, and the wake distribution along the height cannot be ignored unconditionally. From the X–Z view, the serious wake-influenced range narrowed with the increase of the Y distance from the wind turbine position, and the minimum distance between any two wind turbines should be no less than $4D$. Considering the wake effect on each wind turbine's incoming wind is also of great importance. From the X–Y view, the wind distributions at different heights were not symmetrical to the wind turbine hub height plane, and each horizontal plane had a unique distribution of the wake boundary and the wake intensity.

The study concludes that the 3-D wake model is a reliable tool to describe the wind distribution. As for its simplicity, the wake model also makes a potential contribution to wind farm height optimization and nonuniform wind farm layout optimization problems. To more complete the 3-D wake model at the present stage, some additional research should be further conducted. The proper function to simulate the incoming wind distribution is significant; in this study, an exponential function was chosen, which may be the one reasons for the error in the incoming wind, and it may be not the best function. The exponential function also complicates the calculation to some extent. Therefore, a more accurate and simple function to replace the present exponential function is required. In addition, some parameters in the 3-D wake model should be adjusted to fit in different operating conditions. The published measurement data is not enough to conduct an in-depth study of the proposed model. Therefore, some new wind tunnel tests and wind field experiments will be conducted in the near future to determine the parameters and complete this 3-D wake model's validation.

Acknowledgment

The work described in this paper was supported by the Research Institute for Sustainable Urban Development (RISUD) with account number of BBW8 and the FCE Dean Research project with account number of ZVHL, The Hong Kong Polytechnic University.

Reference

[1] K. Rados, G. Larsen, R. Barthelmie, W. Schlez, B. Lange, G. Schepers*, et al.*, "Comparison of wake models with data for offshore windfarms," *Wind Engineering,* vol. 25, pp. 271-280, 2001.

[2] M. Samorani, "The wind farm layout optimization problem," in *Handbook of wind power systems*, ed: Springer, 2013, pp. 21-38.

[3] L. Amaral and R. Castro, "Offshore wind farm layout optimization regarding wake effects and electrical losses," *Engineering Applications of Artificial Intelligence,* vol. 60, pp. 26-34, 4// 2017.

[4] E. Ela, M. Milligan, B. Kirby, Eamonn Lannoye, D. Flynn, M. O'Malley*, et al.*, "Evolution of Operating Reserve Determination in Wind Power Integration Studies," presented at the IEEE Power & Energy Society General Meeting, Minneapolis, Minnesota, 2010.

[5] P. Wang, L. Goel, Y. Ding, and L. P. Chang, "Reliability-based long term hydro/Thermal reserve allocation of power," presented at the IEEE Power & Energy Society General Meeting, 2009.

[6] P. Hou, W. Hu, M. Soltani, and Z. Chen, "A novel energy yields calculation method for irregular wind farm layout," in *Industrial Electronics Society, IECON 2015-41st Annual Conference of the IEEE*, 2015, pp. 000380-000385.

[7] D. R. VanLuvanee, "Investigation of observed and modeled wake effects at Horns Rev using WindPRO," Master, Department of Mechanical Engineering, Fluid Mechanics Section, Technical University of Denmark, 2006.

[8] T. Sørensen, M. L. Thøgersen, P. Nielsen, and N. Jernesvej, "Adapting and calibration of existing wake models to meet the conditions inside offshore wind farms," *EMD International A/S. Aalborg,* 2008.

[9] B. Pérez, R. Mínguez, and R. Guanche, "Offshore wind farm layout optimization using mathematical programming techniques," *Renewable Energy,* vol. 53, pp. 389-399, 2013.

[10] W. Tong, S. Chowdhury, J. Zhang, and A. Messac, "Impact of different wake models on the estimation of wind farm power generation," in *12th AIAA Aviation Technology, Integration, and Operations (ATIO) Conference and 14th AIAA/ISSMO Multidisciplinary Analysis and Optimization Conference*, 2012, p. 5430.

[11] J. Schmidt and B. Stoevesandt, "The impact of wake models on wind farm layout optimization," in *Journal of Physics: Conference Series*, 2015, p. 012040.

[12] J. F. Ainslie, "Calculating the flowfield in the wake of wind turbines," *Journal of Wind Engineering and Industrial Aerodynamics,* vol. 27, pp. 213-224, 1988.

[13] S. Ott, J. Berg, and M. Nielsen, "Linearised CFD models for wakes," *Risø National Laboratory, Roskilde, Denmark,* 2011.

[14] G. C. Larsen, H. Madsen Aagaard, F. Bingöl, J. Mann, S. Ott, J. N. Sørensen*, et al.*, "Dynamic wake meandering modeling," Risø National Laboratory 8755036023, 2007.

[15] L. Manuel, P. S. Veers, and S. R. Winterstein, "Parametric models for estimating wind turbine fatigue loads for design," *Journal of solar energy engineering,* vol. 123, pp. 346-355, 2001.

[16] M. Churchfield, "A review of wind turbine wake models and future directions," in *Proceedings of the North American Wind Energy Academy Symposium (NAWEA'13)*, 2013.

[17] J. Cao, T. Wang, H. Long, S. Ke, and B. Xu, "Dynamic loads and wake prediction for large wind turbines based on free wake method," *Transactions of Nanjing University of Aeronautics and Astronautics,* vol. 32, pp. 240-249, 2015.

[18] B. Hu, "Design of a Simple Wake Model for the Wind Farm Layout Optimization Considering the Wake Meandering Effect," Tech. Rep.(TU Delft, 2016)2016.

[19] A. Niayifar and F. Porté-Agel, "Analytical modeling of wind farms: A new approach for power prediction," *Energies,* vol. 9, p. 741, 2016.

[20] N. Charhouni, "Qualification of three analytical wake models," *S12 Fiabilité et robustesse des systèmes mécaniques,* 2015.

[21] N. O. Jensen, *A note on wind generator interaction*, 1983.

[22] R. Shakoor, M. Y. Hassan, A. Raheem, and Y.-K. Wu, "Wake effect modeling: A review of wind farm layout optimization using Jensen's model," *Renewable and Sustainable Energy Reviews,* vol. 58, pp. 1048-1059, 5// 2016.

[23] N. P. Dufresne and M. Wosnik, "Velocity deficit and swirl in the turbulent wake of a wind turbine," *Marine Technology Society Journal,* vol. 47, pp. 193-205, 2013.

[24] L. P. Chamorro and F. Porté-Agel, "A wind-tunnel investigation of wind-turbine wakes: boundary-layer turbulence effects," *Boundary-layer meteorology,* vol. 132, pp. 129-149, 2009.

[25] M. Bastankhah and F. Porté-Agel, "A new analytical model for wind-turbine wakes," *Renewable Energy,* vol. 70, pp. 116-123, 10// 2014.
[26] L. L. Tian, W. J. Zhu, W. Z. Shen, N. Zhao, and Z. W. Shen, "Development and validation of a new two-dimensional wake model for wind turbine wakes," *Journal of Wind Engineering and Industrial Aerodynamics,* vol. 137, pp. 90-99, Feb 2015.
[27] X. Gao, H. Yang, and L. Lu, "Optimization of wind turbine layout position in a wind farm using a newly-developed two-dimensional wake model," *Applied Energy,* vol. 174, pp. 192-200, 2016.
[28] Y. Chen, H. Li, K. Jin, and Q. Song, "Wind farm layout optimization using genetic algorithm with different hub height wind turbines," *Energy Conversion and Management,* vol. 70, pp. 56-65, 2013/06/01/ 2013.
[29] J. Feng and W. Z. Shen, "Design optimization of offshore wind farms with multiple types of wind turbines," *Applied Energy,* vol. 205, pp. 1283-1297, 2017/11/01/ 2017.
[30] E. W. Peterson and J. P. Hennessey Jr, "On the use of power laws for estimates of wind power potential," *Journal of Applied Meteorology,* vol. 17, pp. 390-394, 1978.
[31] Wikipedia. *Wind profile power law*. Available: https://en.wikipedia.org/wiki/Wind_profile_power_law
[32] R. J. Barthelmie, G. Larsen, S. Frandsen, L. Folkerts, K. Rados, S. Pryor*, et al.*, "Comparison of wake model simulations with offshore wind turbine wake profiles measured by sodar," *Journal of Atmospheric and Oceanic Technology,* vol. 23, pp. 888-901, 2006.
[33] R. J. Barthelmie, S. T. Frandsen, M. N. Nielsen, S. C. Pryor, P. E. Rethore, and H. E. Jorgensen, "Modelling and measurements of power losses and turbulence intensity in wind turbine wakes at Middelgrunden offshore wind farm," *Wind Energy,* vol. 10, pp. 517-528, Nov-Dec 2007.
[34] A. Crespo and J. Herna, "Turbulence characteristics in wind-turbine wakes," *Journal of wind engineering and industrial aerodynamics,* vol. 61, pp. 71-85, 1996.
[35] W. Schlez, A. Tindal, and D. Quarton, "GH wind farmer validation report," Garrad Hassan and Partners Ltd, Bristol,2003.
[36] Y.-T. Wu and F. Porté-Agel, "Large-eddy simulation of wind-turbine wakes: evaluation of turbine parametrisations," *Boundary-layer meteorology,* vol. 138, pp. 345-366, 2011.